

Transient Hamiltonian chaos in the cavity electrodynamics

Kirill N. Alekseev^{(a)*} and Gennady P. Berman^(b)

^(a)*Theory of Nonlinear Processes Laboratory,*

Kirensky Institute of Physics, Krasnoyarsk 660036, Russia

^(b)*Center for Nonlinear Studies, Los Alamos National Laboratory, Los Alamos, New Mexico 87545, USA*

The chaotic dynamics at the interaction between an ensemble of two-level atoms with an eigenmode of a high- Q Fabry-Perot cavity and with an external amplitude-modulated field is considered. It is shown that in the case of an exact atom-field resonance and at the initial population of the atomic ground state, a Hamiltonian chaos in the system is transient. The difference in the chaotic dynamics for a Fabry-Perot and for a ring cavity geometries, as well as the conditions for the experimental observation of the transient Hamiltonian chaos are discussed.

I. INTRODUCTION

Tavis-Cummings (TC) model [1] which describes within the rotating-wave approximation (RWA) [2] the interaction between an ensemble of the two-level atoms with a high- Q cavity mode is a fundamental for quantum and nonlinear optics. Recently the basic dynamic effects predicted for the model have become available for the experimental verification (see [3,4] and references therein).

Belobrov, Zaslavsky and Tartakovsky [5] showed that within the semiclassical approximation a breakdown of the RWA leads to the dynamical chaos (see also [6]). However, for the typical transitions in the optical and in the microwave domains, the violation of the RWA may occur only at rather high atom's density, when a gas model of the noninteracting two-level atoms is not more adequate.

Nowadays other generalizations of the semiclassical TC-model with the Hamiltonian chaos in the RWA appeared [7-13]. These models describe the interaction of the three-level atoms with two cavity modes [7,8], and two-level atoms with one mode and with an external field injected into a cavity with a constant amplitude¹ [9-11], or with the amplitude-modulated field [12]. For the last two cases, the interaction with an external field was taken into account within a standard spatially - homogeneous field approximation ("mean field model") [15].

The common feature of all mentioned above models is the consideration of the sample shorter than the wavelength of the ring cavity with the only forward propagating wave. For the Fabry-Perot cavity, an account of spatial variation of the cavity field amplitude due to the interference between the forward and backward propagating waves may influence sufficiently on the nonlinear characteristics of the atoms-field interaction. This fact has been well appreciated in the theory of optical bistability (see [16, 17] and references therein).

In this paper we are concerned within a semiclassical approach the influence of the standing wave effects on the transition to the Hamiltonian chaos at the interaction between the two-level atoms with the field. We use the model [12], but instead of a ring cavity a Fabry-Perot cavity geometry is considered.

It is shown, that in the simplest case of an exact atom-field resonance and at the initial population of the atomic ground state, the coupled Maxwell-Bloch system is reduced to the Hamiltonian system with 1.5 degrees of freedom — a periodically forced "Bessel pendulum". Conditions for the transition to the dynamical chaos are found numerically. For the majority of the values of the external field amplitude and frequency, chaos is transient: the chaotic oscillations of the population difference and of the polarization become regular after some time. In contrast to other models of physical systems possessing the transient Hamiltonian chaos (see, e. g. [18 - 23]), in our case the effective potential of the Hamiltonian system with 1.5 degrees of freedom is of a multi-well type. This leads to rather complicated nonlinear dynamics of the system. In particular, a time interval of chaotic behavior has complicated dependence on the system's parameters. For trajectories with rather long chaotic part, a sensitivity of a character of settling of a regular oscillations of a cavity field with respect to small variations of the initial conditions or the parameters of the system is found.

The paper is organized as follows. In Sec. 2 we introduce the model describing the dynamics of the system "two-level atoms + field". The ansatz reducing the Maxwell-Bloch system to one equation of periodically driven "Bessel pendulum" in the case of the exact resonance and for some initial conditions is also considered in this Section. In

¹Note that this model may also describe the interaction of impurity center in a crystal with the light and phonons [14]. In such case a cavity is absent.

Sec. 3 after a brief review on the transient Hamiltonian chaos, we describe the nonlinear dynamics of our system. In conclusion, in Sec. 4 we compare the particularities in the dynamics of atoms-field interaction for a geometry of the Fabry-Perot and ring cavities, and discuss the possibilities of the experimental observation of the transient Hamiltonian chaos, and also point out some open problems.

II. MODEL

Our system consists of N identical two-level atoms with a transition frequency ω_0 and a dipole matrix element d , interacting with the radiation field mode with the frequency $\omega \approx \omega_0$. The sample with atoms of the length L and the volume V completely fills a high- Q Fabry-Perot cavity ($-L \leq z \leq 0$). An external amplitude-modulated field E_{ext} is injected into the cavity at the plane $z = 0$. The field has the form

$$E_{ext} = E_0 F(t) \cos \omega t, \quad (1)$$

where $F(t)$ is a periodic function of time ($|F(t)| = 1$) slowly varying in comparison with the carrier frequency ω . In this paper we shall consider the simplest type of modulation $F(t) = \sin \Omega t$, but it can be expected that the main results are also applicable for the case, when the modulation $F(t)$ consists of many harmonics. Following the classical paper of Spencer and Lamb [24], we shall consider the influence of an external field as a small local perturbation preserving a cavity mode structure of the form

$$E_{SC}(z, t) = E(t) \sin(kz), \quad (2)$$

where $k = n\pi L^{-1}$ is the wave number of the chosen n -th cavity mode. The dynamics of atoms is described by the Bloch equations

$$\begin{aligned} \dot{S}_1(z, t) &= -\omega_0 S_2(z, t), \\ \dot{S}_2(z, t) &= \omega_0 S_1(z, t) + \frac{2d}{\hbar} E_{SC}(z, t) S_3(z, t), \\ \dot{S}_3(z, t) &= -\frac{2d}{\hbar} E_{SC}(z, t) S_2(z, t), \end{aligned} \quad (3)$$

$$S_1^2 + S_2^2 + S_3^2 = 1, \quad (4)$$

where the pseudospin variables S_i ($i = 1, 2, 3$) are connected with the probability amplitudes for the population of upper a_j and lower b_j levels of the j -th atom [9, 12, 25]

$$\begin{aligned} S_1(z, t) &= \frac{1}{N_s} \sum_{j \in \Delta V}^{N_s} (a_j^* b_j + a_j b_j^*), \\ S_2(z, t) &= -\frac{i}{N_s} \sum_{j \in \Delta V}^{N_s} (a_j^* b_j - a_j b_j^*), \\ S_3(z, t) &= \frac{1}{N_s} \sum_{j \in \Delta V}^{N_s} (|a_j|^2 - |b_j|^2). \end{aligned} \quad (5)$$

In (5) $\Delta V = (\Delta z)\pi r^2$ is a small averaging volume, z is the coordinate of slice center with the width $\Delta z \ll \lambda$ (λ is wavelength), r is a characteristic radius of the sample with a gas of atoms, N_s is the number of atoms in the volume ΔV ($N_s \gg 1$).

The behavior of the field inside the cavity is governed by the Maxwell equation including an influence of the external field [24]

$$\begin{aligned} \ddot{E}(t) + \omega^2 E(t) &= -4\pi \ddot{P}(t) - \frac{2\omega c}{L} E_{ext}, \\ \tilde{P}(t) &= \frac{2}{L} \int_{-L}^0 dz P(z, t) \sin(kz), \end{aligned} \quad (6)$$

where $P(z, t)$ is a polarization of the two-level medium determined by

$$P(z, t) = \frac{N}{V} dS_1(z, t). \quad (7)$$

The coupled Maxwell-Bloch system (3), (6), (7) completely describes the dynamics on the time interval shorter than all characteristic relaxation times of atoms and field. These equations may be simplified by separation of fast and slow dynamics. For this purpose make a transformation into the rotating system of coordinates

$$\begin{aligned} S_1(z, t) &= u(z, t) \cos(\omega t) - v(z, t) \sin(\omega t), \\ S_2(z, t) &= u(z, t) \sin(\omega t) + v(z, t) \cos(\omega t), \\ S_3(z, t) &= w(z, t), \end{aligned} \quad (8)$$

and introduce the envelopes of the self-consistent field in the following way

$$E(t) = E_1(t) \cos(\omega t) + E_2(t) \sin(\omega t). \quad (9)$$

Assume that the conditions of a slow variance of the envelopes in a comparison with the carrier frequency ω

$$\begin{aligned} |\dot{u}| \ll \omega |u|, \quad |\dot{v}| \ll \omega |v|, \quad |\dot{w}| \ll \omega |w|, \\ |\dot{E}_{1,2}| \ll \omega |E_{1,2}|, \end{aligned} \quad (10)$$

are valid. Then, substituting (1), (8) into (3), (6), (7) and using the RWA and a slowly varying envelope approximation (SVEA) [2] one can derive the following equations

$$\begin{aligned} \dot{u} &= \Delta v + w\mathcal{E}_2 \sin(kz), \\ \dot{v} &= -\Delta u + w\mathcal{E}_1 \sin(kz), \\ \dot{w} &= -(u\mathcal{E}_2 + v\mathcal{E}_1) \sin(kz) \\ \dot{\mathcal{E}}_1 &= \omega_c^2 \frac{2}{L} \int_{-L}^0 dz v(z, t) \sin(kz) + GF(t), \\ \dot{\mathcal{E}}_2 &= \omega_c^2 \frac{2}{L} \int_{-L}^0 dz u(z, t) \sin(kz). \end{aligned} \quad (11)$$

In (11) $\Delta = \omega - \omega_0$ is a detuning from the optical resonance, $G = (c\epsilon_0)/L$, $\mathcal{E}_j = dE_j/\hbar$ ($j = 0, 1, 2$), $\omega_c = (2\pi N d^2 \omega_0 / \hbar V)^{1/2}$ is a so-called cooperative frequency [26] characterizing the time of energy transfer between atoms and field in the absence of the external field ($E_0 = 0$).² The Maxwell-Bloch equations possess the pseudospin length conservation law

$$u(z, t)^2 + v(z, t)^2 + w(z, t)^2 = 1. \quad (12)$$

Substituting (8) into (7), we obtain the representation for the polarization via the slow variables u and v

$$P(z, t) = \frac{Nd}{V} [u(z, t) \cos(\omega t) - v(z, t) \sin(\omega t)]. \quad (13)$$

The condition of applicability of the RWA and the SVEA may be written in the form

$$\max(G^{1/2}, \omega_c, \Omega) \ll \omega \sim \omega_0. \quad (14)$$

As a rule, for typical optical and microwave systems this condition is valid.

Now the system (11) contains only slow variables. To solve it, it is necessary to define the initial spatial distributions of polarization components $u(z, t = 0) \equiv u_0(z)$ and $v_0(z)$ as well as population difference $w_0(z)$ and field envelopes $\mathcal{E}_{1,2}(0)$. Deriving a general solution of (11) looks as rather difficult problem, so we consider only particular solution for an exact resonance and at the specific initial condition.

²In modern literature also notions such as ‘‘collective Rabi frequency’’ and ‘‘vacuum- field Rabi frequency’’ are used for the determination of this frequency (see the discussion of the corresponding terminological questions in [4]).

It may be shown that for an exact resonance ($\Delta = 0$), if $u(z, t = 0) = \mathcal{E}_2(t = 0) = 0$, then $u(z, t) = \mathcal{E}_2(t) = 0$ for any t .³ In this case it follows from (12) that the polarization $v(z, t)$ and the population difference $w(z, t)$ may be parameterized by one angle variable $\phi(z, t)$

$$\begin{aligned} v(z, t) &= -\sin \phi(z, t), \\ w(z, t) &= -\cos \phi(z, t). \end{aligned} \quad (15)$$

Introduce the following ansatz

$$\begin{aligned} \phi(z, t) &= \vartheta(t) \sin(kz), \\ \vartheta(t) &= \int_0^t dt' \mathcal{E}_1(t'). \end{aligned} \quad (16)$$

From (15) one can derive

$$\begin{aligned} v(z, t) &= -2\sum_{n=0}^{\infty} J_{2n+1}(\vartheta(t)) \sin[(2n+1)kz], \\ w(z, t) &= -J_0(\vartheta(t)) - 2\sum_{n=0}^{\infty} J_{2n}(\vartheta(t)) \cos(2nkz), \end{aligned} \quad (17)$$

where $J_n(x)$ is the Bessel function. In these notations the equations (11) may be transformed to one equation of the periodically driven ‘‘Bessel pendulum’’

$$\begin{aligned} \ddot{\vartheta} + 2\omega_c^2 J_1(\vartheta) &= G \sin \Omega t, \\ \dot{\vartheta} &= \mathcal{E}_1 \equiv \mathcal{E}(t). \end{aligned} \quad (18)$$

Taking into account that for small x : $J_1(x) \approx x/2$, one can see that the cooperative frequency ω_c is just the frequency of small oscillations of the pendulum at $G = 0$.

As far as we know, the ansatz (16), (17) was first introduced in [27] when studying the metastable states in the coupled ‘‘atoms + field’’ system. The equation of the ‘‘Bessel pendulum’’ without the external driving ($G = 0$) has been also obtained in [27].

Now we discuss the problem of the limits of applicability of the ansatz (16), (17). Expansion (17) should be correct for any $v(z, t)$ and $w(z, t)$ including the initial distribution $v_0(z)$ and $w_0(z)$. It means that should exist such $\vartheta(0) \equiv \vartheta_0$, for which the expansions

$$\begin{aligned} v_0(z, t) &= -2\sum_{n=0}^{\infty} J_{2n+1}(\vartheta_0) \sin[(2n+1)kz], \\ w_0(z, t) &= -J_0(\vartheta_0) - 2\sum_{n=0}^{\infty} J_{2n}(\vartheta_0) \cos(2nkz), \end{aligned} \quad (19)$$

are identities.⁴ But the fulfillment of (19) is possible not for all $v_0(z)$ and $w_0(z)$. Among the initial distributions $v_0(z)$ and $w_0(z)$ for which (19) is correct, there are at least two physically significant cases: (i) the case of the periodic δ -like distribution and the population difference corresponding to $\vartheta_0 \gg 1$, and (ii) the case of spatially homogeneous and weak initial excitation of two-level medium $w_0(z) \approx -1$ and $v_0(z) \approx 0$. Such initial distribution corresponds to $\vartheta_0 \approx 0$. Note that ansatz (16), (17) can be used for any initial values of the field $\mathcal{E}(0)$.

In what follows, we shall consider physically most interesting case of atoms initially populated in the ground state ($w_0(z) = -1$, $v_0(z) = 0$), and when initially the field in the cavity is absent ($\mathcal{E}(0) = 0$). It means that for the pendulum (18), the initial conditions are fixed: $\vartheta(0) = \dot{\vartheta}(0) = 0$.

III. HAMILTONIAN DYNAMICS

Equation (18) may be written in the Hamiltonian form

$$\begin{aligned} \frac{d\vartheta}{d\tau} &= \frac{\partial H}{\partial p}, \quad \frac{dp}{d\tau} = -\frac{\partial H}{\partial \vartheta}, \\ H &= p^2/2 + V(\vartheta) - \overline{G}\vartheta \sin(\overline{\Omega}\tau), \\ V(\vartheta) &= -2J_0(\vartheta), \end{aligned} \quad (20)$$

³Or, if $v(z, t = 0) = \mathcal{E}_1(t = 0) = 0$, then $v(z, t) = \mathcal{E}_1(t) = 0$ for any t .

⁴Prof. Wei-Mou Zheng called our attention to this fact.

where $p \equiv \mathcal{E}/\omega_c$, $\tau = \omega_c t$, $\bar{G} = G/\omega_c^2$, $\bar{\Omega} = \Omega/\omega_c$. The form of potential $V(\vartheta)$ is shown in Fig. 1.

Transfer into extended phase space [28] and introduce a pair of new canonically conjugated variables (ψ, I) according to the formulas

$$\begin{aligned} \frac{d\psi}{d\tau} &= \frac{\partial \tilde{H}}{\partial I}, & \frac{dI}{d\tau} &= -\frac{\partial \tilde{H}}{\partial \psi}, \\ \psi &= \bar{\Omega}\tau & \tilde{H} &= H + \bar{\Omega}I. \end{aligned} \quad (21)$$

The new Hamiltonian \tilde{H} is the integral of motion in the extended phase space (ϑ, p, ψ, I) . We used formulas (21) to control the errors in the numerical calculations.

In spite of rather simple form of the equation (18), the dynamics of this Hamiltonian system with 1.5 degrees of freedom may be very complicated. Such a behavior is due to the form of the potential $V(\vartheta)$ which is not periodic, and is a decreasing function of ϑ at $|\vartheta| \rightarrow \infty$. Under the influence of a periodic forcing both regular and chaotic dynamics are possible. As $V(\vartheta) \rightarrow 0$ at $\vartheta \rightarrow \pm\infty$, then the asymptotic behavior of the dynamics is regular. Therefore, among with trapped periodic and chaotic trajectories, transient chaos is possible.

In recent years the investigations on the transient Hamiltonian chaos attract considerable attention (see, e. g., reviews [18,19] and references therein). The majority of papers deal with the study of particle scattering on $2D$ or $3D$ potentials [18-20]. It was quite recently realized that stochastic ionization of atoms and molecules or, generally speaking, any escape of chaotic trajectory from the potential well are also examples of the transient Hamiltonian chaos. The transient chaos under the conditions of stochastic ionization is not only much more poorly studied, but also is organized more complicated than chaos in the potential scattering [22]. This is due to the fact that the phase space structure of the typical Hamiltonian systems is not uniform: Along with the stochastic seas the great number of islands with the stable dynamics are presented, which are the source of the trajectory trapping for a long time.

In paper [21] the stochastic ionization of kicked Morse oscillator is considered. Initial oscillator's state corresponds to the potential minimum. It was shown, that the time of chaotic escape from the well t_{esc} may be sensitive to a small change of the parameters of the system. The boundaries of the regions with the different t_{esc} are fractals in the space of parameters: amplitude — period of external driving.

In paper [23] the escape of chaotic trajectory from $2D$ potential has been studied. It was shown that for strong chaos the directions and time of escape from the well are significantly sensitive to a small change of the initial conditions. The region in the space of the initial conditions corresponding to the trajectory escape during a fixed number of iterations appears to be a fractal.

All mentioned above papers were devoted to the study of chaotic escape from $2D$ potential (2 degrees of freedom), or from $1D$ potential which consists of one potential well (1.5 degrees of freedom). The particularity of our system with 1.5 degrees of freedom consists in multi-well structure of the effective potential (see Fig. 1). It should be noticed also, that in our case initial conditions are fixed just in the bottom of the first well.

There may exist several types of the trajectories (both trapped and unbounded): stable periodic, unstable periodic, trapped chaotic and unbounded chaotic demonstrating transient chaos. Due to nonlocal structure of our effective potential, the trajectory can be trapped not only within the first (central) well, but inside other wells too. Of course, time interval of trajectory trapping inside different wells is quite different. Trapped chaotic trajectories exist only for some singular values of parameters and the most typical behavior is transient chaos. During transient chaotic motion trajectory after escaping from the first well may randomly visit several wells and be trapped within these wells for some time. So, because of nonlocal character of the effective potential, transient chaotic motion may be organized rather complicated.

We illustrate now the main types of the nonlinear dynamics. First, if the conditions of chaos are not satisfied, then a trajectory is located in the first well ($-3.83 \leq \vartheta \leq 3.83$) forever. A corresponding form of the field (momentum of effective system (20)) for regular motion is shown in Fig. 2. Under the conditions of chaos the behavior of the system is more various:

- (a) An example of unstable quasiperiodic trajectory trapped inside first (central) well during all time of computation is shown in Figs. 3, 4. Such trajectories are observed mainly for the parameter values belong to the vicinity of the chaos boundary.
- (b) Examples of transient chaos are shown in Figs. 5 and 6. The trajectory quickly escapes from first well, visits randomly and “rotates” during some time inside few other wells and, by the end, a regular asymptotic motion sets in. (Note that minimums of the wells correspond to the values $\vartheta \approx 0, \pm 7, \pm 13.3, \pm 19, \pm 25$ etc.). The signs of the coordinate ϑ and the momentum p setting in at $t \rightarrow \infty$ are random. Very small variation of the initial conditions leads to absolutely different asymptotic state (compare Figs. 5 and 6). This results is the interesting physical effect: the small fluctuations of the initial cavity field produce the change of the asymptotic field state sign (Fig. 7).

(c) An example of chaotic trajectory trapped during all time of computation is shown in Fig. 8. The trajectory quickly escapes from the first well ($\tau_{esc} \approx 10.8$), then visits few neighbor wells and again returns to the first well. Corresponding chaotic field oscillations are shown in Fig. 9.

(d) By the other hand, a transition to the regular behavior may be very quick and just after escaping from first well (Figs. 10, 11).

The regions of regular and chaotic behavior in the space of parameters: amplitude of driving — frequency of modulation are shown in Fig. 12. The chaos boundary is marked by stars, the regularity windows lying near this boundary are marked by boxes. The minimal value of the external field amplitude ($\overline{G} \approx 0.14$) leading to chaos was observed at the frequency $\overline{\Omega} \approx 0.85$. The trajectories with chaotic parts of different length exist in the regions situated above the chaos boundary. These trajectories have positive maximal Lyapunov exponent during the time interval of chaotic motion. Our preliminary numerical simulations show rather complicated dependence of the length of the chaotic phase on the parameters. But definitely the trajectories with long chaotic path ($\tau_{esc} \sim 10^2$), as a rule, belong to the layer with the width ~ 0.1 near the boundary with the chaotic component.

We also studied the sensitivity of the sign of the self-consistent field asymptotic state with respect to the small variation of the external field amplitude. The results are presented in Fig. 13. Dimensionless perturbation parameter \overline{G} was changing in the region $[0.89, 0.9]$ with a step 10^{-4} . A regular asymptotic state with a positive field ($\mathcal{E} > 0$) is displayed by plus one (+1), and the opposite case of the negative field ($\mathcal{E} < 0$) is marked by minus one (-1). It is seen from Fig. 13, that in some regions of the perturbation parameter values \overline{G} , the sign of the asymptotic field state is sensitive to small variation of \overline{G} . Such kind of behavior is characteristic for trajectories with rather long chaotic path ($\tau_{esc} \approx 40 \div 100$).

In concluding part of this section we compare spatial structure of polarization and population difference at regular and chaotic dynamics (see formula (17)). An essential contribution into the expansion (17) make only spatial harmonics with the index of the Bessel functions less than its argument. For regular dynamics, the argument of Bessel function ϑ is smooth regular function of time. In this case the spatial spectrum of v and w may contain many harmonics, but the energy transfer between different spatial modes is regular. By contrast, for chaotic temporal dynamics ϑ is random function of time. As a consequence, spatial chaos in the distribution of the population difference and polarization appears.

IV. DISCUSSION

It is interesting to compare a nonlinear dynamics of the system of two-level atoms + self-consistent field + external amplitude-modulated field for different geometry of the cavity. Generalized coupled Maxwell-Bloch system may be reduced to the periodically driven “Bessel pendulum” (18) in the case of the Fabry - Perot cavity. For the majority of parameter values, Hamiltonian chaos is transient in this system. By contrast, for the ring cavity, the dynamics of the system within the same approximation is governed by the equation of the periodically driven physical pendulum [12]

$$\ddot{\vartheta} + \omega_c^2 \sin \vartheta = GF(t),$$

where $\vartheta(t)$ is the Bloch angle. Due to periodicity of the corresponding potential $V(\vartheta) = -\omega_c^2 \cos \vartheta$ and for periodic $F(t)$, the dynamical chaos is stationary. Appearance of the transient chaos is possible only for a special choice of $F(t)$, i. e. when $F(t)$ contains zero harmonic [12]. Then, the effective potential loses its translation invariance.

At present time the oscillatory energy transfer between atoms and field has been observed in both optical and microwave domains [4]. Present here some estimates. For dipole transition with $d \sim 1$ Debye and atom’s density 10^{14}cm^{-3} , the value of the cooperative frequency $\omega_c \sim 10^{10} \text{s}^{-1}$ may be large then the dissipative rates associated with the atom relaxation and cavity losses. We believe that the rapid progress in the experimental cavity quantum electrodynamics makes observation of the transient Hamiltonian chaos accessible.

In summary, we considered the influence of the spatial structure of a standing wave on the chaotic dynamics in the interaction of an ensemble of two-level atoms with the field. It is shown, that for the majority of parameter values, chaos is transient. For trajectories with long chaotic path, the asymptotic behavior of the field is sensitive to small variation of the initial conditions and parameters. Temporal chaos has manifestation in the spatial behavior of the polarization and of the population difference.

In conclusion we point out some relevant problems for future research. First, a complicated nonlinear dynamics of periodically forced “Bessel pendulum” deserves more detail and deep study in the frameworks of general problem of transient chaos. Second, the problem of influence of quantum effects on chaos in potential scattering attracts great attention of researches (see review [29]). But the influence of quantum effects on the other types of the

transient Hamiltonian chaos is yet not considered. So, it could be interesting to study the influence of the cavity field quantalization on the transient chaos in the model discussed.

ACKNOWLEDGEMENTS

We thank P.W. Milonni for discussion and V. S. Egorov for sending us a reprint of the paper [27]. One of us, A. K. N. , also acknowledges Hao Bai-Lin and Wei-Mou Zheng for hospitality, support and useful discussions during his visit of ITP (Beijing), where a big part of this work was done.

* E-mail: kna@iph.krasnoyarsk.su
E-mail: kna@vist.krascience.rssi.ru

1. Tavis M., Cummings F. W., Phys. Rev. 1968. V.170. P.379.
2. Allen L., Eberly J. H., *Optical Resonance and Two-Level Atoms*, New York: Wiley, 1975.
3. Hughey B. J., Gentile T. R., Kleppner D., Phys. Rev. A. 1990. V.41. P.6245.
4. Meschede D., Phys. Rept. 1992. V.211. P.201. sec. 6.2.2 .
5. Belobrov P. I., Zaslavsky G. M., Tartakovskiy G. Kh., Sov. Phys. JETP. 1976. V.44. P.945 .
6. (a) Milloni P. W., Ackerhalt J. R., Galbraith H. W., Phys. Rev. Lett. 1983. V.50. P.966; (b) Munz M., Z. Phys. B. 1983. V.53. P.311; (c) Graham R., Höhnerbach M., Z. Phys. B. 1984. V.57. P.233; (d) Nath A., Ray D. S., Phys. Rev. A. 1987. V.36. P.431; (e) Eidson J. C., Fox R. F., Phys. Rev. A. 1986. V.34. P.482 and P.3288; (f) Graham R., Höhnerbach M., *Quantum Measurement and Chaos.*, Ed. by E. R. Pike and S. Sarkar, New York: Plenum Publ., 1987. P.147.
7. Shepelyansky D. L., Phys. Rev. Lett. 1986. V.57. P.1815.
8. Harms K.-D., Haake F., Z. Phys. B. 1990. V.79. P.159.
9. Alekseev K. N., Berman G. P., Sov. Phys. JETP. 1987. V.65. P.1115.
10. Holm D. D., Kovacic G., Sundaram B., Phys. Lett. A. 1991. V.154. P.346.
11. Holm D. D., Kovacic G., Physica D. 1992. V.56. P.270.
12. Alekseev K. N., Berman G. P., Sov. Phys. - JETP. 1988. V.67. P.1762.
13. Alekseev K. N., Berman G. P., Holm D. D., *Hamiltonian Optical Chaos: Classical, Semiclassical and Quantum*, 1993, to be published.
14. Alekseev K. N., Alekseeva N. V., Phys. Lett. A. 1992. V.162. P.82.
15. Bonifacio R., Lugiato L. A., Phys. Rev. A. 1978. V.18. P.1129.
16. Carmichael H. J., Herman J. A., Z. Phys. B. 1980. V.38. P.365.
17. Carmichael H. J., *Optica Acta*. 1980. V. 27. P.147.
18. Smilansky U., *Chaos and Quantum Physics*, Ed. by M.-J. Giannoni, A. Voros and J. Zinn-Justin, Amsterdam: Elsevier, 1991.
19. Tel T., *Experimental Study and Characterization of Chaos (Directions in Chaos V.3)*, Ed. by Hao Bai-Lin, Singapore: World Scientific, 1990. P.149.
20. Bleher S., Grebogi C., Ott E., Physica D. 1990. V.46. P.87.
21. Heagy J. F., Lu Z.-M., Yuan J.-M., Vallieros M., *Quantum Non - Integrability (Directions in Chaos, V.4)*, Ed. by Da Hsuan Feng, Jian-Min Yuan, Singapore: World Scientific, 1992. P.322.
22. Pikovsky A., J. Phys. A.1992. V.25. P. L477.
23. Contopoulos G., Kandrup H. E., Kaufman D., Physica D. 1993. V.64. P.310.
24. Spencer M. B., Lamb W. E., Phys. Rev. A. 1972. V.5. P.884.
25. Polder D., Schurmans M. F. H., Vreken Q. H. F., Phys. Rev. A. 1972. V.19. P.1192.
26. (a) Kazantsev A. P., Smirnov V. S., Sov. Phys. - JETP. 1964. V.19. P.130; (b) Alekseev A. I., Vdovin Yu. A., Galitzky V.M., Sov. Phys. - JETP. 1964. V.19. P.220.

27. Egorov V. S., Chekhonin I. A., Zh. Thech. Phys. 1986. V.56. P.572. [Sov. Phys. - Tech. Phys. 1986 V. 31 P. 344]
28. Lichtenberg A., Liberman M. A., *Regular and Stochastic Motion* New York: Springer, 1983, chap. 1.
29. Blümel R., *Quantum Non - Integrability (Directions in Chaos, V.4)*, Ed. by Da Hsuan Feng, Jian-Min Yuan — Singapore: World Scientific, 1992. P.397.

FIGURE CAPTIONS

Figure 1. The form of the potential for the Bessel pendulum $V(x) = -2J_0(x)$.

Figure 2. Dependence of the self-consistent field $p \equiv \mathcal{E}/\omega_c$ on time for regular motion inside the first potential well: $\overline{G} = 0.8$; $\overline{\Omega} = 1.3$.

Figure 3. Weakly unstable chaotic orbit of length $\tau = 200$ located in the first well: $\overline{G} = 0.271$; $\overline{\Omega} = 0.8$.

Figure 4. Dependence of the field on time. The values of parameters are the same as in Fig. 3.

Figure 5. Trajectory of the length $\tau = 200$ under the conditions of the transient chaos ($\overline{G} = 0.7$; $\overline{\Omega} = 0.6$).

Figure 6. Same as Fig. 5, but with slightly changed initial conditions for the field: $p(0) = 10^{-4}$.

Figure 7. Changing of the asymptotic field state at small variation of the initial conditions. Process marked by boxes corresponds to the initial condition $p(0) = 0$, not marked process — $p(0) = 10^{-4}$. Values of parameters are the same as in Figs. 5 and 6.

Figure 8. Chaotic trajectory of length $\tau = 200$ at $\overline{G} = 0.6$; $\overline{\Omega} = 0.9$.

Figure 9. Chaotic field oscillations for the parameter values are the same as in Fig. 8.

Figure 10. Quick escape from the first potential well ($\tau_{esc} = 14.8$) and setting of the regular motion at $\overline{G} = 0.4$; $\overline{\Omega} = 0.9$.

Figure 11. Dependence of the field on time. Values of parameters are the same as in Fig. 10.

Figure 12. Regions of regular and chaotic motion in parameter space: amplitude — frequency.

Figure 13. The influence of the variation of the driving amplitude on the sign of the asymptotic field state (for explanation, see main text), $\overline{\Omega} = 0.4$.

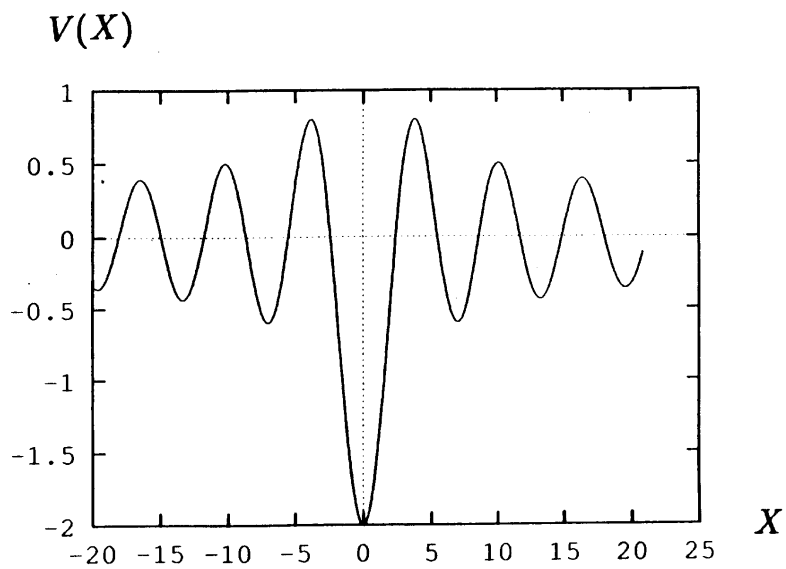


Fig. 1

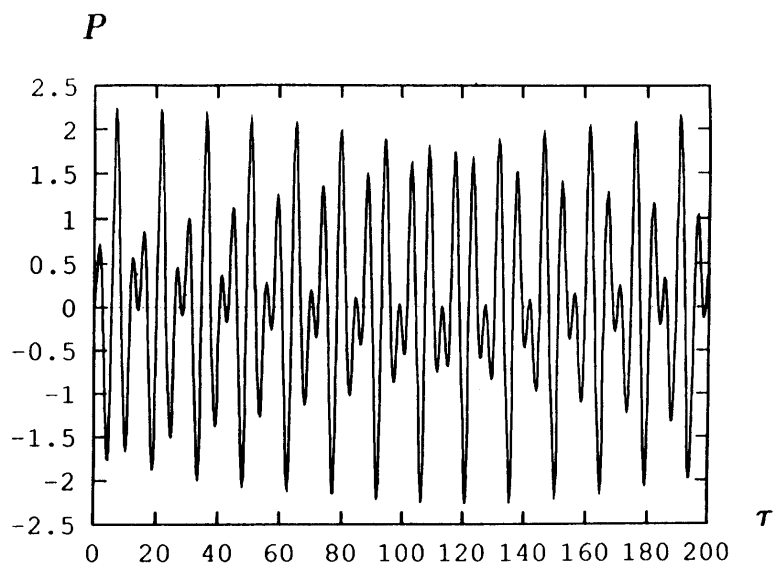


Fig. 2

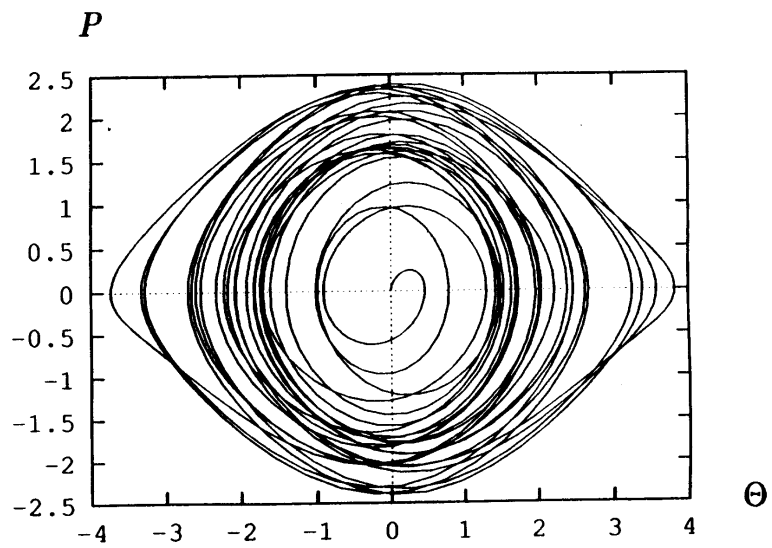


Fig. 3

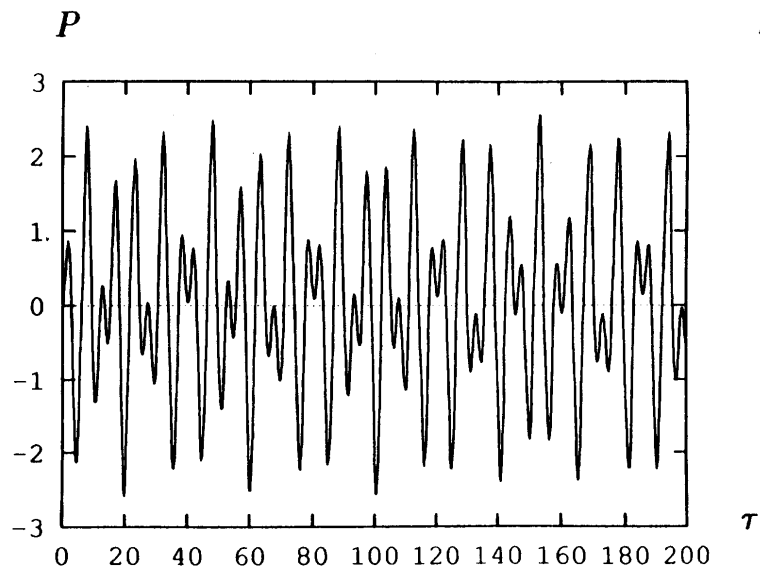


Fig. 4

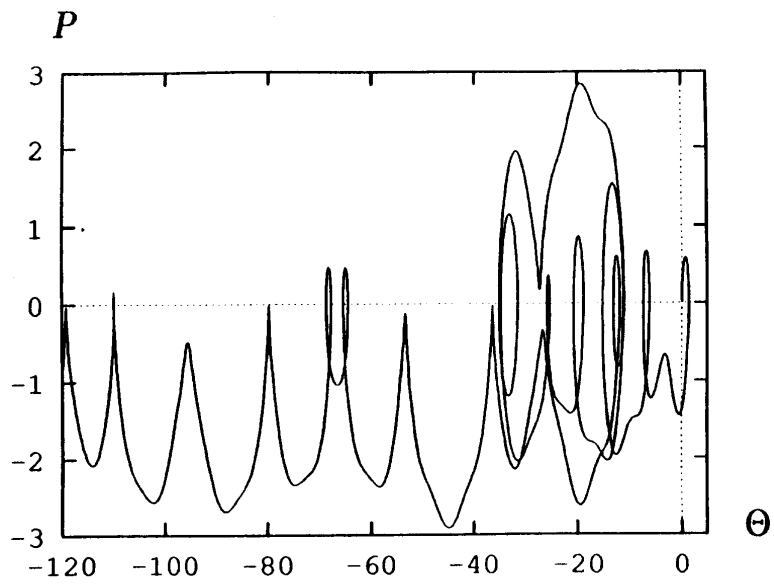


Fig. 5

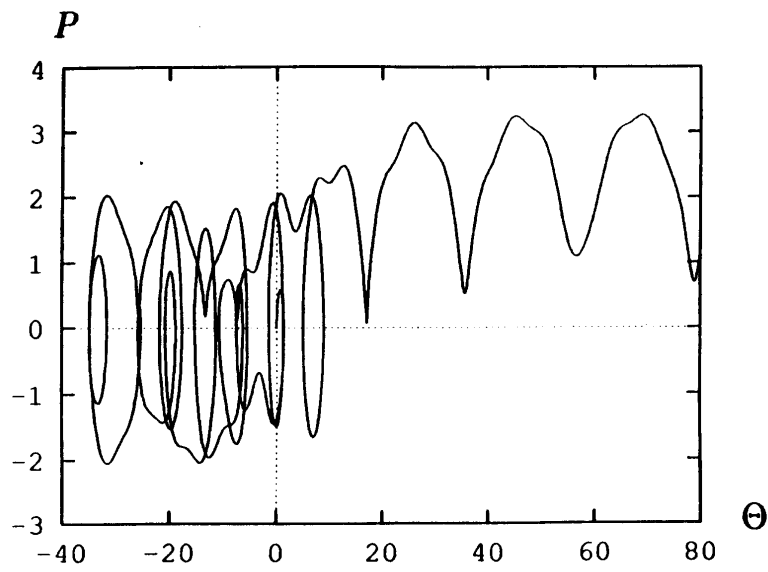


Fig. 6

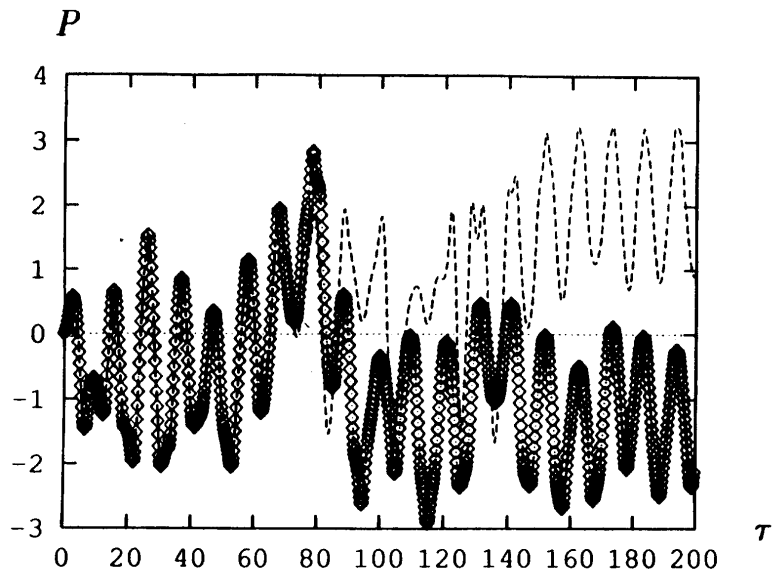


Fig. 7

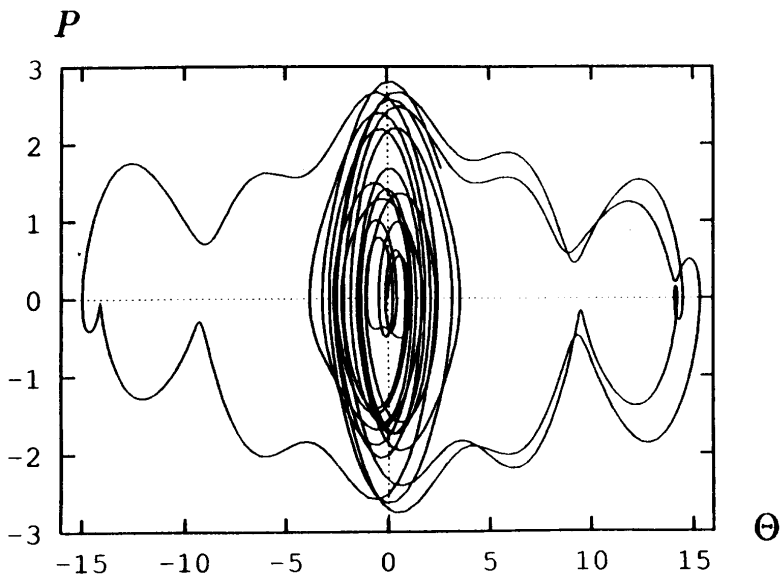


Fig. 8

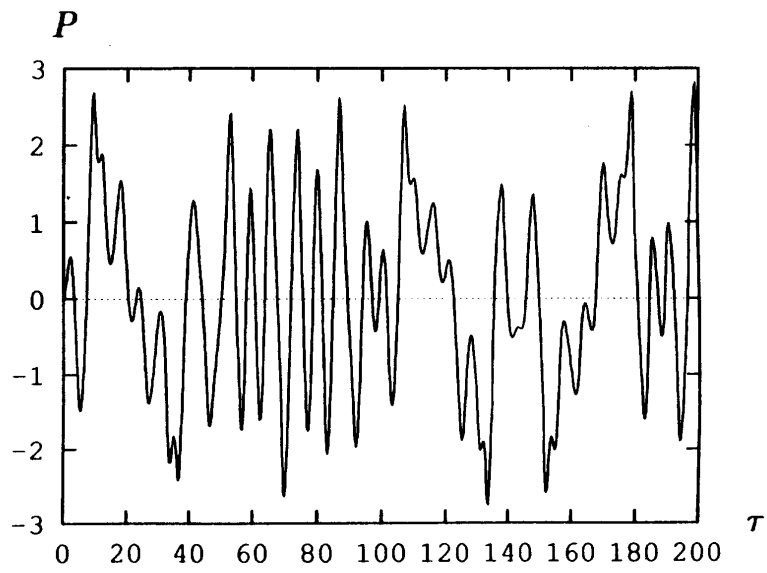


Fig. 9

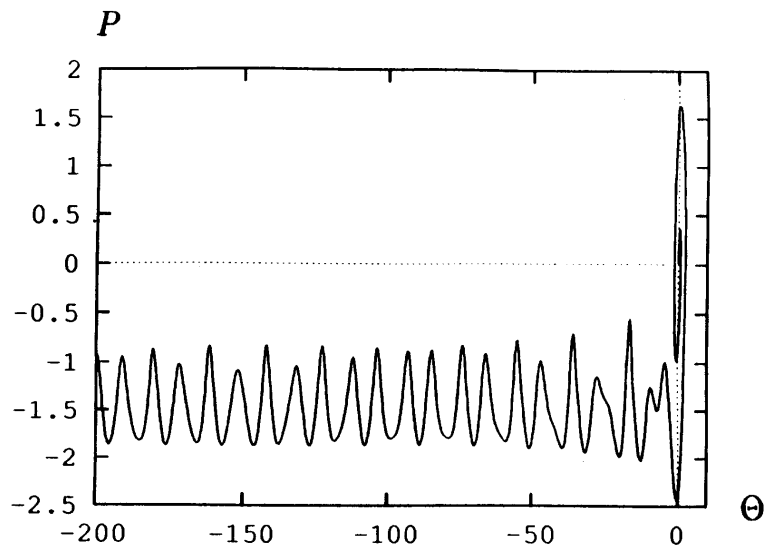


Fig. 10

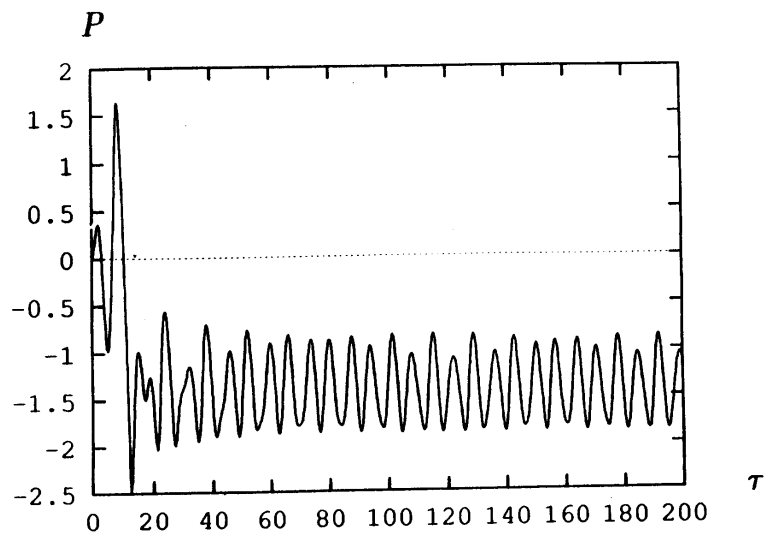


Fig. 11

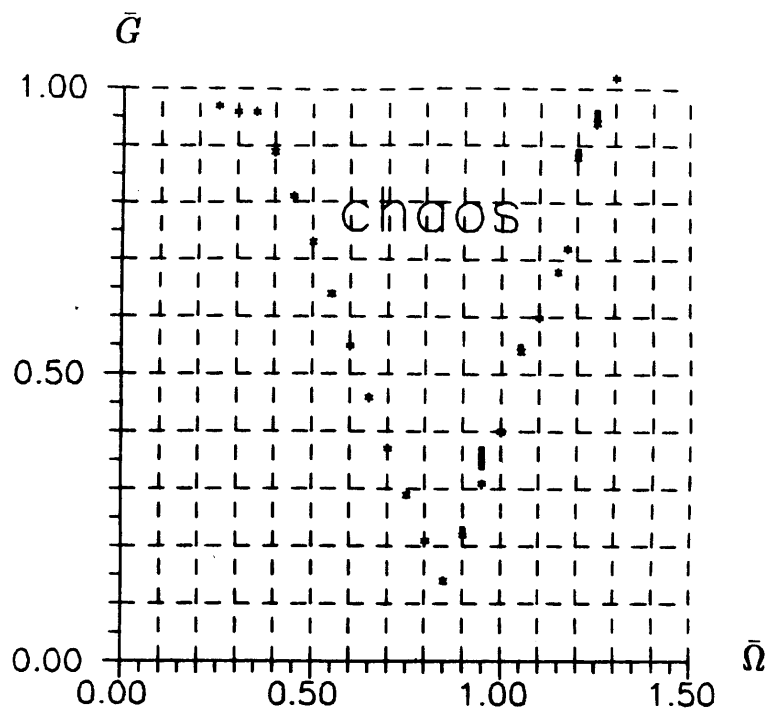


Fig. 12

$Sign(P)_\infty$

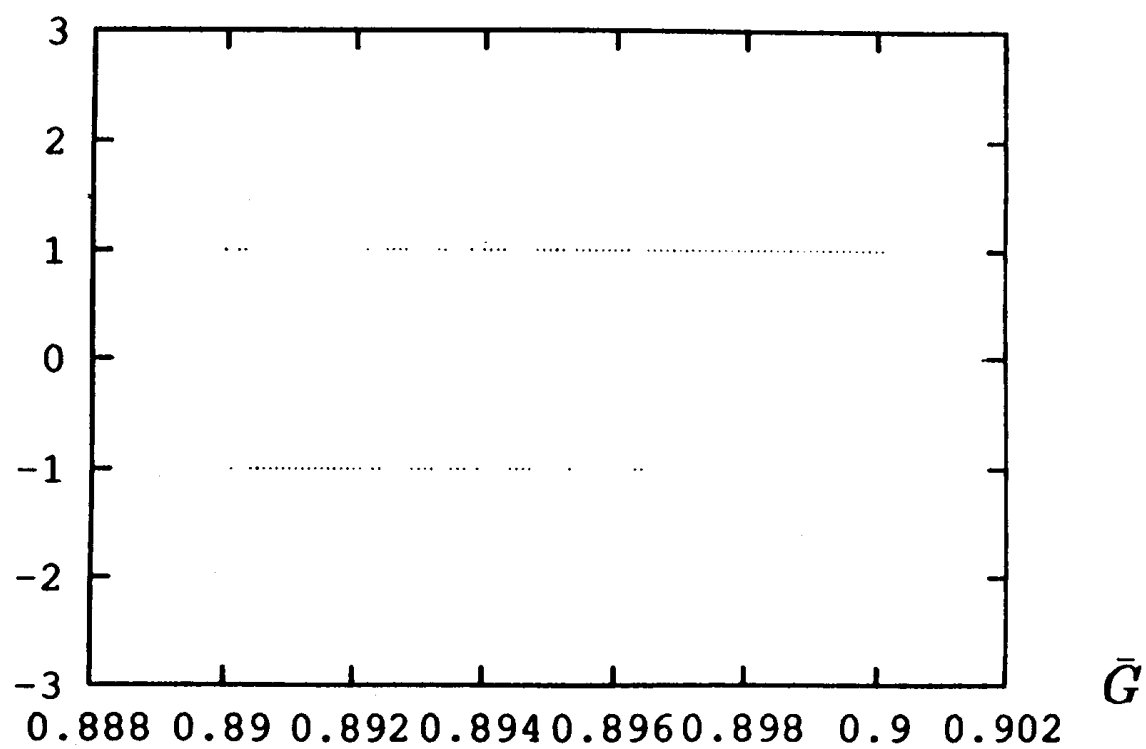


Fig. 13